

NUMERICAL STUDY OF TURBULENT FLOW OVER CIRCULAR STRIP ROUGHNESS IN OPEN CHANNEL

By Jian LIU*, Akihiro TOMINAGA** and Masashi NAGAO***

A low Reynolds number k- ϵ turbulence model is used to predict the turbulent flow over circular strip roughness in open channel. Non-rectangular meshes are employed for treatment of the irregular boundaries near the circular roughness elements. The turbulence characteristics in response to the roughness spacing is predicted. The influence of configuration of the roughness element on the flow is studied. The calculated results are compared with the experimental data. The maximum of the turbulence kinetic energy contour is at the upstream corner of the roughness element. The mixing effects of the flow become strong with a decrease of the relative spacing. The resistance coefficient takes maximum value at the relative spacing of $L/H_r = 8$.

Keywords: strip roughness, non-rectangular meshes, relative spacing, resistance coefficient.

1. INTRODUCTION

The flow over roughness boundary is one of the most interesting fluid motions in practical engineering. Therefore, many studies on the flow over rough boundary have been carried out experimentally and numerically by using various kinds of roughness elements. As we have known, discussing the turbulence structure of the flow over strip roughness is one of the approaches to understand the generation mechanism of turbulence in the flow over rough boundary. According to Knight and Macdonald¹⁾, the spacing between roughness elements has important influence on resistance coefficient compared with the height of roughness element for the flow over strip roughness; the resistance coefficient attains maximum when the relative spacing L/H_r defined as the ratio of the spacing L between the roughness elements and the roughness height H_r is from 6 to 10. If the relative spacing is smaller than 6, there are dead water regions between the roughness elements, and the height responded by the flow is smaller than the actual one; on the other hand, when the spacing of strip roughness is very large, it is easy to understand that resistance is smaller since the quantity of roughness elements is small in the total flow area. Tominaga and Nezu²⁾ and Tominaga³⁾ conducted measurements on turbulence in open channel flows over circular and rectangular strip roughness, using two-component laser-Doppler anemometer (LDA) Tominaga, et al.⁴⁾ and Liu et al.⁵⁾ evaluated the turbulence structure over square strip roughness in open channel by using a low Reynolds number (LRN) k- ϵ model which is a modified version of Jones and Launder⁶⁾ model and standard k- ϵ turbulence model, respectively. Comparisons of the velocities calculated with two turbulence models with the experimental data are fairly good. However, the standard k- ϵ model gives the excessive high predictions for turbulent shear stresses, turbulent intensities and resistance coefficient. Although the low Reynolds number k- ϵ model presents adequate results, the calculated turbulent shear stress, turbulent intensity and resistance coefficient are still smaller than the experimental data for the case of $L/H_r = 2$. Recently, Tominaga, et al.⁷⁾ proposed a new LRN k- ϵ turbulence model for flow over square strip roughness in open channel. The predictions by Tominaga, et al.⁷⁾ are better than ones in Ref. 4. But, the simulation of the flow over circular strip roughness has not been made until now.

In the present study, the turbulence model of Tominaga, et al.⁷⁾ is used for predicting the turbulent flow over circular strip roughness in open channel. The calculated results are compared with the experimental data of Tominaga and Nezu²⁾ to check the validity of the turbulence model for predicting the turbulent flow over circular strip roughness in open channel.

Because the boundaries around roughness elements are irregular due to the existence of circular roughness elements (see Fig. 1), special treatment near the solid wall is necessary. The body-fitted transformation is generally applied to treat irregular boundaries, but, after adopting the transformation, some additional terms will be put into the transformed governing equations. Thereby, the amount of calculated work will be increased greatly. Furthermore, it is very difficult to obtain the proper transformation in some cases. Hence, the procedure for treatment of irregular boundaries in Cartesian coordinates developed by Liu et al.⁸⁾ are alternatively applied to treat irregular boundaries in this study.

* M. Eng, Research Engineer, Dept. of Civil Eng., Nagoya Inst. of Tech., Gokiso, Showa, Nagoya 466, Japan

** Member, Dr. of Eng., Assoc. Prof., Dept. of Civil Eng., Nagoya Inst. of Tech., Gokiso, Showa, Nagoya 466, Japan

*** Member, Dr. of Eng., Prof., Dept. of Civil Eng., Nagoya Inst. of Tech., Gokiso, Showa, Nagoya 466, Japan

2. BASIC EQUATIONS & TURBULENCE MODEL

The two-dimensional turbulent flow over circular strip roughness in open channel is described by the Reynolds equations. The variables in the turbulent flow are modeled by a control volume method. The x and y coordinates are chosen in the streamwise direction and the direction normal to the river bed, respectively (see Fig. 1). In the present paper, calculations have been carried out with the turbulence model of Tominaga et al.⁷⁾. The set of elliptic partial differential equations governing mass, momentum, and energy conservation can be written as follows:

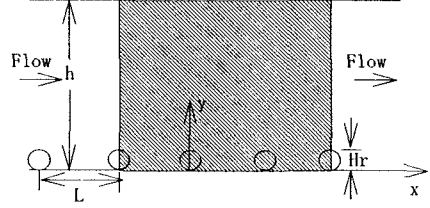


Fig. 1 Schematic diagram of open channel flow over circular strip roughness

$$\frac{\partial}{\partial x}(u\phi) + \frac{\partial}{\partial y}(v\phi) = \frac{\partial}{\partial x}\left(\Gamma_\phi \frac{\partial \phi}{\partial x}\right) + \frac{\partial}{\partial y}\left(\Gamma_\phi \frac{\partial \phi}{\partial y}\right) + S_\phi \quad (1)$$

where ϕ represents different dependent variables, Γ_ϕ stands for generalized diffusion coefficients, S_ϕ is source terms.

The governing equations for the open channel flow over circular strip roughness are represented in Table 1. Variables u and v are the mean velocities in x - and y -directions, respectively, P is the pressure, P_k represents the production of turbulence kinetic energy by the interaction of the mean velocity gradients and turbulent stresses, ρ is the density. Parameter $\nu_{\text{eff}} = \nu + \nu_t$ is the effective viscosity, ν is the kinematic viscosity, ν_t is turbulent viscosity, its value is given by $\nu_t = f_\mu C_\mu k^2/\epsilon$, k is the turbulence kinetic energy and ϵ is the dissipation rate. The empirical coefficients take the values as: $C_\mu = 0.09$, $C_{\epsilon 1} = 1.44$, $C_{\epsilon 2} = 1.92$, $\sigma_k = 1.0$, $\sigma_\epsilon = 1.3$. The functions f_μ , f_1 , f_2 are given as follows⁷⁾:

$$\begin{aligned} f_\mu &= (1 + C_k / \sqrt{\text{Re}_t}) \times [1 - \exp(-a\sqrt{\text{Re}_y} - b\text{Re}_y)] \\ f_1 &= 1.0 \\ f_2 &= [1 - \exp(-\text{Re}_t^2)] \times [1 - \exp(-c\text{Re}_y)] \end{aligned} \quad (2)$$

where $\text{Re}_t = k^2/\nu\epsilon$ and $\text{Re}_y = k^{1/2}y/\nu$ are turbulent Reynolds numbers, y is the distance normal to the solid wall. The constants are given the values as: $a = 0.0115$, $b = 0.0075$, $c = 0.069$ and $C_k = 2.5$.

The boundary condition for the dissipation rate ϵ at the wall is as follows:

$$\epsilon_w = 2\nu \left[\left(\frac{\partial \sqrt{k}}{\partial x} \right)^2 + \left(\frac{\partial \sqrt{k}}{\partial y} \right)^2 \right] \quad (3)$$

Because of the configuration of the roughness element being circular, it is very difficult to treat the irregular boundary near the bed. Moreover, the LRN turbulence model requires many grid nodes near solid wall, so the real circular section of the roughness element is replaced by the form shown in Fig. 2 in the process of calculations, that is, the semi-circular configuration of the roughness element near the bed is replaced by the rectangle of $H_r \times 0.5H_r$. The arc boundaries near the upper part of roughness element are treated by using the method developed by Liu et al.⁸⁾ in the present study.

The appearance of the boundary layer requires a non-equidistant grid system along the walls. The sides of the control volumes near the solid walls are positioned in y direction and in front and back of the roughness elements in x direction according to geometrical progression. 70% of grids are located between the bed and the level of two times of roughness height in y -direction.

The equations in Table 1 are discretized on rectangular and non-rectangular control volumes⁸⁾. The hybrid scheme is used to discretize the convection terms. The pressure field is calculated by using the SIMPLE method of Patankar⁹⁾. The discretized equations are solved by a tridiagonal matrix algorithm (TDMA). Some under-relaxation are required to prevent divergence of the iteration process. The criterion of convergence of numerical solution is on the basis of the absolute normalized residuals of the equations. The solutions are regarded as converged values when these normalized residuals become less than 5×10^{-6} for all variables.

Because Eq. (1) is elliptic, it is necessary to define the boundary conditions for all variables on all boundaries of the flow domain. At the wall, no-slip condition is used. At the inlet, the variables are taken from log-law profiles, while zero gradients can be set at the outlet. At the free-surface, the symmetry conditions are employed except for turbulence energy which is modified by introducing a dumping factor to consider the effect of damping of turbulence⁴⁾. The regions which locate in the roughness elements are treated by means of the method of extension of computational region proposed by

Table 1 Governing equations for the open channel flow over circular strip roughness

Equation	ϕ	Γ_ϕ	S_ϕ
Continuity	1	0	0
x- momentum	u	ν_{eff}	$-\frac{\partial P}{\rho \partial x} + \frac{\partial}{\partial x} \left(\nu_{eff} \frac{\partial u}{\partial x} \right) + \frac{\partial}{\partial y} \left(\nu_{eff} \frac{\partial v}{\partial x} \right)$
y- momentum	v	ν_{eff}	$-\frac{\partial P}{\rho \partial y} + \frac{\partial}{\partial x} \left(\nu_{eff} \frac{\partial u}{\partial y} \right) + \frac{\partial}{\partial y} \left(\nu_{eff} \frac{\partial v}{\partial y} \right)$
k	k	$\nu + \nu_t/\sigma_k$	$P_k - \epsilon$
ϵ	ϵ	$\nu + \nu_t/\sigma_\epsilon$	$f_1 C_{\epsilon 1} P_k \epsilon/k - f_2 C_{\epsilon 2} \epsilon^2/k$
$P_k = \nu_t \left[2 \left(\frac{\partial u}{\partial x} \right)^2 + 2 \left(\frac{\partial v}{\partial y} \right)^2 + \left(\frac{\partial u}{\partial y} + \frac{\partial v}{\partial x} \right)^2 \right]$			

Patankar⁹⁾. The computational area shown in Fig. 1 is chosen such that the inlet and the outlet are located at the center of the roughness elements. The calculated ranges in streamwise direction for different relative spacing L/Hr are about 20 times of water depth.

3. PRESENTATION AND DISCUSSION

The various cases shown in Table 2 are numerically simulated by using the aforementioned k- ϵ turbulence model. In Table 2, the diameter Hr of the circular roughness element is equal to 8mm. Relative spacing L/Hr is changed from 1, 2, 4, 8, 16 up to infinity which means that only one roughness element exists in the flow. The flow depth h is measured from the bed, the relative depths h/Hr are equal to 10 for all cases. The Reynolds number Re and the Froude number Fr are defined by $Re = U_m h/\nu$ (U_m is the mean bulk velocity) and $Fr = U_m/\sqrt{gh}$ (g is the gravitational acceleration), respectively. Without specific notification in this section, the predicted and measured values are non-dimensional. The calculated results are compared with the experimental data of Tominaga and Nezu²⁾.

Table 2 Hydraulic conditions

Case	L/Hr	h/Hr	U_m (cm/s)	Re	Fr
Rk01	∞	10	27.40	20000	0.31
Rk03	16	10	25.56	18200	0.29
Rk05	8	10	23.4	16500	0.26
Rk08	4	10	25.10	17400	0.29
Rk10	2	10	32.07	20900	0.37
Rk12	1	10	40.15	25200	0.47

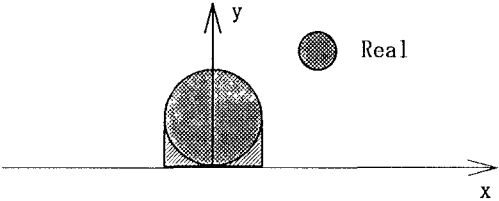


Fig. 2 Treatment of configuration of roughness element

Fig. 3 and Fig. 4 show the streamwise velocity and the Reynolds stress distributions for the cases of $L/Hr \geq 16$ and $L/Hr \leq 2$, based on the calculated values and experimental data ($x/Hr = 0$ is at the center of the roughness element). The computed velocities are in good agreement with the measurements except for the over-prediction of about 10% in the vicinity of roughness elements for the cases of $L/Hr \leq 2$. The agreement of the calculated Reynolds stresses with the experimental data is very good, except for having some errors near the front roughness element for the case of $L/Hr = 16$. The distributions of the Reynolds stresses $-uv/U_m^2$ vary linearly in the region far from the bed. The values of $-uv/U_m^2$ near the bed change rapidly, especially, the variation of $-uv/U_m^2$ in y -direction for the case of $L/Hr = \infty$ is most remarkable. Moreover, with the decrease of L/Hr , the peaks of $-uv/U_m^2$ become smaller and smaller until it reaches the minimum value at the case of $L/Hr = 1$.

Fig. 5 shows the comparison of the calculated and measured variations of turbulence intensities u'/U_m for the cases of

$L/Hr \geq 16$ and $L/Hr \leq 2$. Since only the turbulent kinetic energy k is calculated in the present $k-\epsilon$ model, u' is evaluated by the formula of $u' = 0.744\sqrt{2k}$ according to Nezu et al.¹⁰⁾. The calculated turbulence intensities agree well with the experimental data except for having some errors near the bed and roughness elements. The calculated values for the case of $L/Hr = 16$ are larger than the experimental data in the vicinity of the downstream side of the front roughness elements. This might be related to the method of the treatment of the irregular boundary near the bed and the scope of application of $u' = 0.744\sqrt{2k}$.

The turbulence kinetic energy contour for the case of $L/Hr = 16$ is shown in Fig. 6. The maxima are at the upstream corners of the roughness elements. This phenomenon is the same as that of the flow over square strip roughness in open channel⁴⁾. A second maximum occurs the downstream of the front roughness element.

Fig. 7 is a comparison of the resistance coefficient f ($=8(u_*'/U_m)^2$, u_*' is the friction velocity which is calculated by the Reynolds stress) with the experimental data. It is also given that the f of the open channel flow over square strip roughness obtained by Tominaga and Nezu³⁾, in which the relative water depth is equal to 10. The predicted values tally with the experimental data except for the case of $L/Hr = 8$. The calculated resistance coefficient f for the case of $L/Hr = 8$ is slightly larger than the experimental f . The resistance coefficient takes maximum value at $L/Hr = 8$. This result is identical with the experimental data. It is also found that the varying tendency of the f of the flow over circular strip roughness in open channels is the same as one of the open channel flow over square strip roughness. The effect of configuration of roughness element on the resistance coefficient is not sharp.

4. CONCLUSIONS

The $k-\epsilon$ turbulence model proposed by Tominaga et al.⁷⁾ is used for predicting the turbulent flow over circular strip roughness in open channel. The predictions are examined against experimental data²⁾. Good agreement is obtained for all cases, in which prediction for the resistance coefficient is the best. Further researches to the turbulence model and the treatment of irregular boundary near the bed are needed to better predict the Reynolds stress, turbulence intensity.

From above-mentioned results, with the variation of the roughness spacing, the parameters of the turbulence characteristics in the vicinity of the roughness elements vary distinctly. For the cases of $L/Hr \leq 8$, the resistance of the turbulent flow over circular strip roughness in open channel will decrease with a decrease of the relative spacing. The configuration of roughness element has not important influence on the resistance coefficient under the condition of same relative water depths.

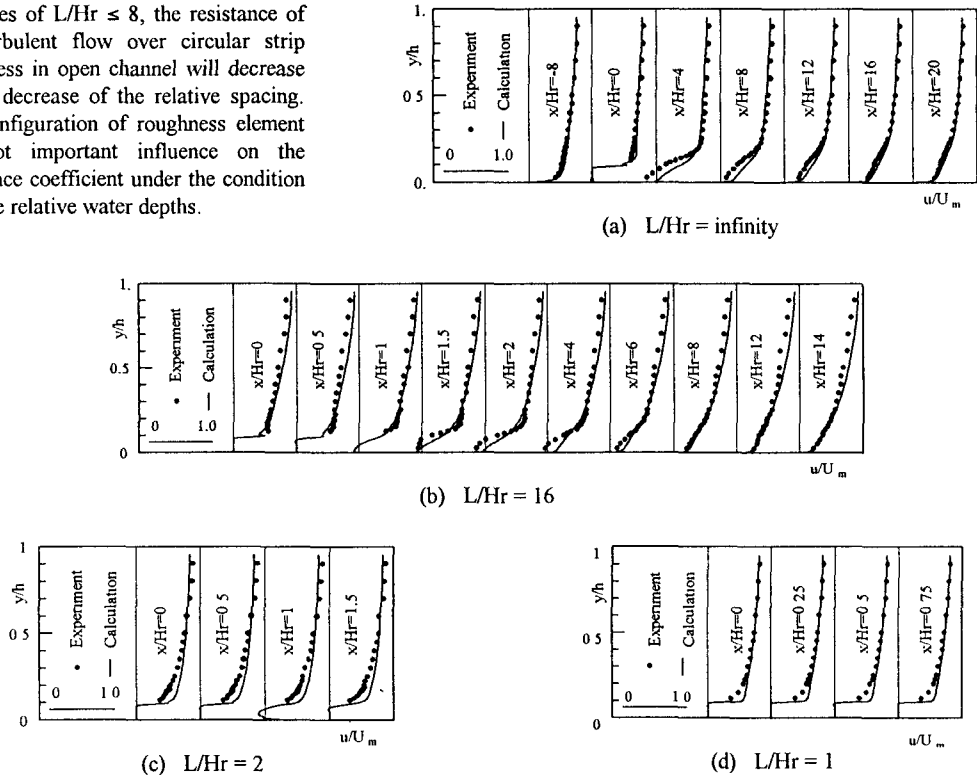


Fig. 3 Comparisons of the calculated velocities with the experimental data for $L/Hr \geq 16$ and $L/Hr \leq 2$

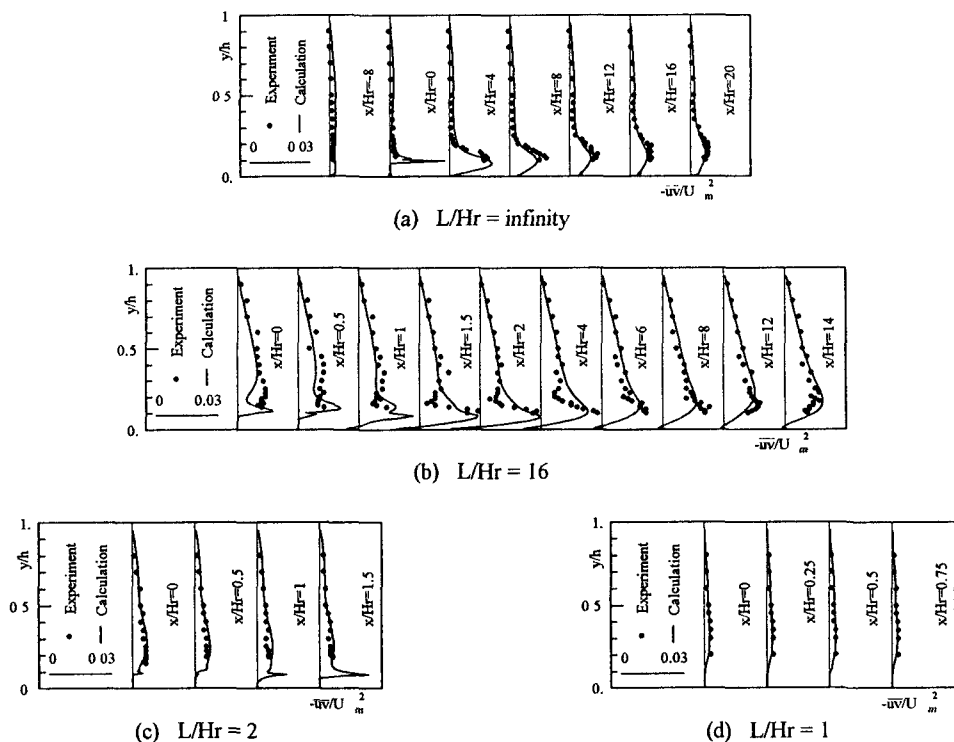


Fig. 4 Comparisons of the calculated Reynolds stresses with the experimental data for $L/Hr \geq 16$ and $L/Hr \leq 2$

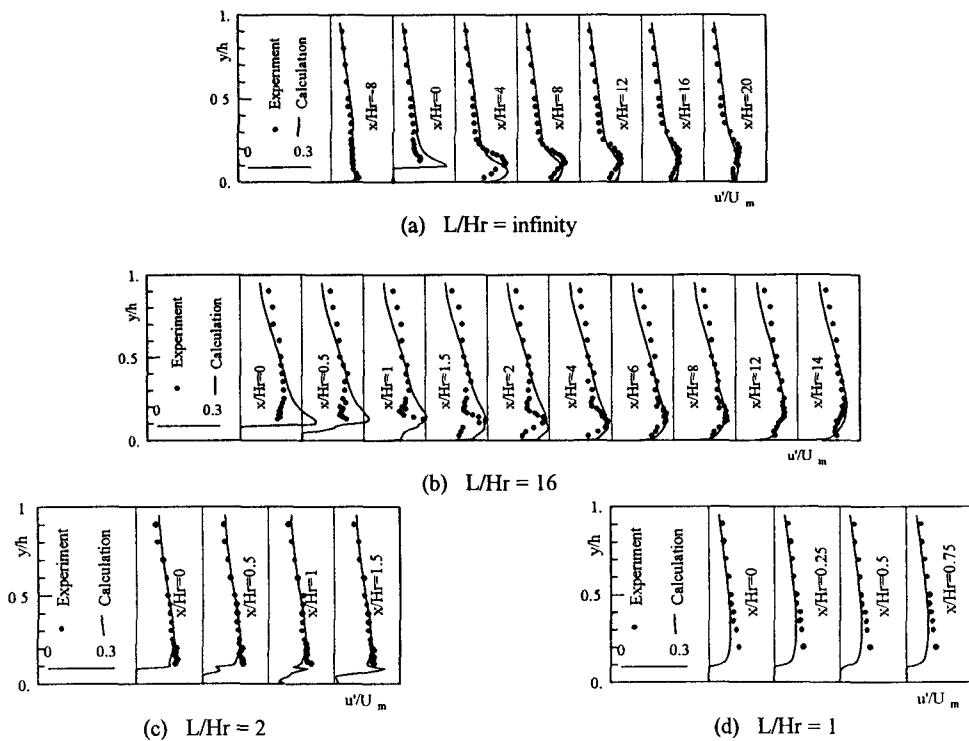


Fig. 5 Calculated and measured turbulence intensities u'/U_m for $L/Hr \geq 16$ and $L/Hr \leq 2$

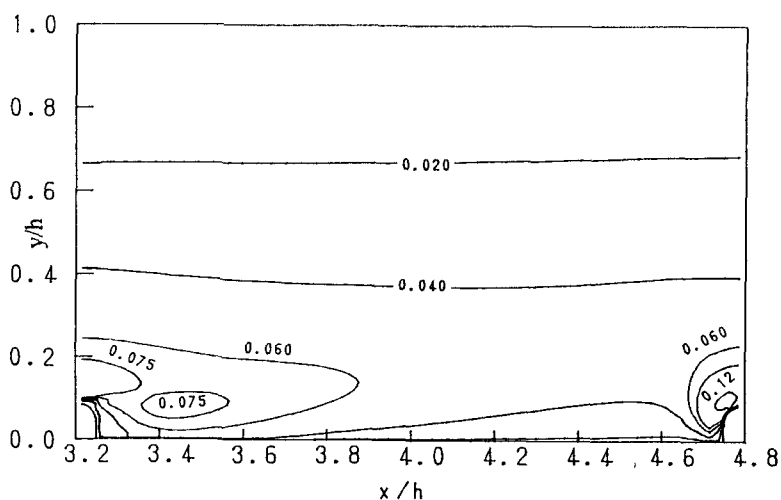


Fig. 6 Turbulence kinetic energy contour for $L/Hr=16$

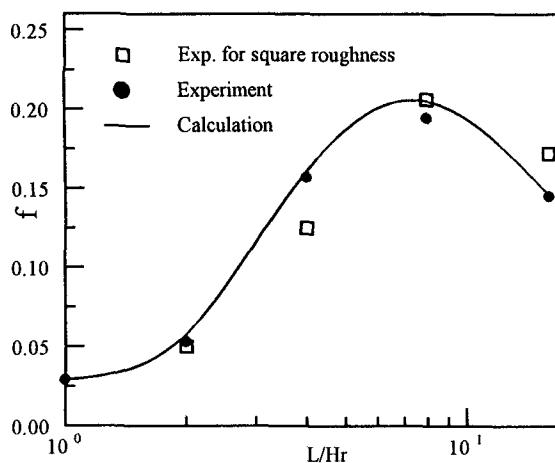


Fig. 7 Comparison of the calculated resistance coefficient with the experimental data

REFERENCES

- 1) Knight, D.W. and Macdonald, J.A., ASCE, Vol.105, Hy-6, pp. 675-690, 1979.
- 2) Tominaga, A. and Nezu, I., Proc. of 24th IAHR Congress, Madrid, pp. c43-c50, 1991.
- 3) Tominaga, A., Proc. of Hydraul. Eng., JSCE, Vol.36, pp.163-168, 1992 (in Japanese).
- 4) Tominaga, A., Liu, J. and Nagao, M., J of Hydraul., Coastal and Environ. Eng., JSCE, No. 521/II-32, pp. 227-237, 1995
- 5) Liu, J., Tominaga, A. and Nagao, M., Hydra 2000 26th IAHR Congress, Vol.1, London, pp. 165-170, 1995.
- 6) Jones, W.P. and Launder, B.E., Int. J. Heat Mass Transfer, Vol.16, pp. 1119-1130, 1972.
- 7) Tominaga, A., Liu, J., Nezu, I. and Nagao, M., Proc. of the Int. Symp. on Mathematical Modelling of Turbulent Flows, Tokyo, Japan, pp. 339-344, Dec., 1995.
- 8) Liu, J., Tominaga, A. and Nagao, M., J. Hydrosci. and Hydraul. Eng., JSCE, Vol.12 No.2, pp. 85-100, 1994.
- 9) Patankar, S.V.: Numerical Heat Transfer and Fluid Flow, Hemisphere, Washington, D.C., 1980.
- 10) Nezu, I., Nakagawa, H. and Tominaga, A., Proc. of 5th Symp. on Refined Flow Modelling and Turbulence Measurements, Paris, pp. 629-636, Sep., 1993.